JOURNAL OF AIRCRAFT
Vol. 31, No. 6, November–December 1994

Separation Control on High-Lift Airfoils via Micro-Vortex Generators

John C. Lin,* Stephen K. Robinson,† and Robert J. McGhee‡
NASA Langley Research Center, Hampton, Virginia 23681
and
Walter O. Valarezo§
McDonnell Douglas Aerospace, Long Beach, California 90846

An experimental investigation has been conducted to evaluate boundary-layer separation control on a two-dimensional single-flap, three-element, high-lift system at near-flight Reynolds numbers with small surface-mounted vortex generators. The wind-tunnel testing was carried out in the NASA Langley Low-Turbulence Pressure Tunnel as part of a cooperative program between McDonnell Douglas Aerospace and NASA Langley Research Center to develop code validation data bases and to improve physical understanding of multielement airfoil flows. This article describes results obtained for small (subboundary-layer) vane-type vortex generators mounted on a multielement airfoil in a landing configuration. Measurements include lift, drag, surface pressure, wake profile, and fluctuating surface heat fluxes. The results reveal that vortex generators as small as 0.18% of reference (slat and flap stowed) wing chord ("micro-vortex generators") can effectively reduce boundary-layer separation on the flap for landing configurations. Reduction of flap separation can significantly improve performance of the high-lift system by reducing drag and increasing lift for a given approach angle of attack. At their optimum chordwise placement on the flap, the micro-vortex generators are hidden inside the wing when the flap is retracted, thus extracting no cruise drag penalty.

Nomenclature

C_d = drag coefficient
C_l = lift coefficient
C_p = pressure coefficient
c = reference airfoil chord (slat and flap stowed)
h = vortex-generator height
L/D = lift-to-drag ratio
M = Mach number
n = normal distance from the surface
Re_c = Reynolds number based on c
x = coordinate along the chord direction
y = vertical distance in the wake profile with origin at the tunnel centerline
α = angle of attack
Δ = differential value
δ = boundary-layer thickness

Subscripts
max = maximum value
∞ = freestream value

Introduction

THE performance of high-lift systems on subsonic transport aircraft plays a major role in determining field-length requirements, payload/range capability for a given field length, and the noise footprint in the airport area during takeoff and landing. High-lift systems have traditionally been mechanically complex, generally consisting of some combination of leading-edge slats and multiple trailing-edge flaps. However, economic pressures are currently pushing modern transport designers toward mechanically simpler high-lift systems with performance equal to or better than older, more complex designs. A current design objective is to reduce the number of flap elements from two or three to one. The main challenge of moving to single-flap designs is to maintain high maximum lift values at landing conditions without incurring boundary-layer separation and the resulting performance losses.[1]

Flow separation on multielement airfoils can be a complicated function of geometry and flight conditions, and is not reliably predictable at this time. For example, previous reports[1–4] have shown that certain high-lift configurations exhibit boundary-layer separation on the flap at low angles of attack, while fully attached flap flow occurs near maximum lift conditions. In these cases, altering the geometrical configuration to avoid low angle-of-attack flap separation had the detrimental effect of reducing maximum lift. In situations like this, one possible means of maintaining high maximum lift values while attenuating boundary-layer separation at low angles of attack is to employ flap-mounted vortex generators to enhance streamwise momentum in the flap upper-surface boundary layer. The question is then to determine what are the smallest vortex generators that provide separation control, and what are their aerodynamic costs?

Conventional, vane-type, passive vortex generators (VGs) with device height h on the order of δ have long been used to increase near-wall momentum through the momentum transfer from the outer flow to the wall region. First introduced by Taylor,[5] these vortex generators consist of a row of small plates or airfoils that project normal to the surface and are set at an angle of incidence to the local flow to produce an array of streamwise trailing vortices. These vortex generators are commonly used to delay boundary-layer separation,[6] to enhance aircraft wing lift,[7–9] and to tailor wing-buffet characteristics at transonic speeds. A wide variety of VGs are

Presented as Paper 92-2636 at the AIAA 10th Applied Aerodynamics Conference, Palo Alto, CA, June 22–24, 1992; received Jan. 17, 1993; revision received March 14, 1994; accepted for publication March 31, 1994.

*Aerospace Engineer, Experimental Flow Physics Branch, Fluid Mechanics Division. Member AIAA.
†Head, Experimental Flow Physics Branch, Fluid Mechanics Division.
‡Head, Low-Turbulence Pressure Tunnel Section, Experimental Flow Physics Branch, Fluid Mechanics Division.
§Principal Specialist, Subsonic Aerodynamics Technology Group; currently at Boeing Commercial Airplane Group.

in use, and most large aircraft employ them for separation control. Many applications, however, use relatively large VGs that cost residual drag through conversion of aircraft forward momentum into unrecoverable turbulence in the aircraft wake. By reducing the height of conventional vane-type vortex generators to only a fraction of δ, vortex generators can still provide wallward momentum transfer over a region several times their own height, especially in high Reynolds number boundary layers. For example, various sub-δ-scale vortex generators were recently shown to significantly reduce the flow separation over a backward-facing ramp.[10] Although sub-δ-scale vortex generators such as Wheeler's wishbones[11] have been shown to control laminar separation bubbles on low Reynolds number airfoils,[12] only vane-type VGs were selected for this investigation since they have been shown to be equal to or better than the Wheeler-type in controlling turbulent boundary-layer separation.[10] Furthermore, these vane-type generators are lighter, less bulky, and can be relatively easy to manufacture in large quantities at NASA Langley.

The objective of the present study was to determine the smallest VGs that would reduce or eliminate separation on a particular two-dimensional single-flap, three-element high-lift system at near-flight Reynolds numbers. An additional practical goal was to determine a size and placement for the vortex generators to allow stowage within the flap well during cruise, to avoid any cruise drag penalty.

Experimental Apparatus

Langley Low-Turbulence Pressure Tunnel Test Facility

The experimental results presented in this article were obtained from tests conducted in the Langley Low-Turbulence Pressure Tunnel (LTPT). The LTPT is a single-return, closed-circuit wind tunnel that can be operated at total pressures ranging from near-vacuum to 10 atm.[13] A diagram of the tunnel-circuit layout is shown in Fig. 1. The LTPT has centerline turbulence intensity levels of 0.034% operating at a Mach number of 0.20 and a total pressure of 60 psi. The contraction ratio is 17.6:1 and the test section is 3 ft wide, 7.5 ft high, and 7.5 ft long. The tunnel can achieve a maximum Reynolds number of 15×10^6/ft at a Mach number of 0.22, although all the testing reported here was conducted at a freestream Mach number M_∞ of 0.20, and Re_c of 5 and 9×10^6. These two Reynolds numbers represent typical three-dimensional wind-tunnel and flight conditions at the critical wing station for low-speed stall for a narrow body transport, respectively.

To ensure spanwise uniformity of the flowfield when testing relatively low aspect-ratio high-lift airfoils near maximum lift conditions, some form of tunnel sidewall boundary-layer control (BLC) is needed. The large adverse pressure gradients induced on the tunnel sidewalls by the airfoils can cause the sidewall boundary layer to separate with a corresponding loss of spanwise uniformity of the flow on the airfoil surfaces. A suction system employing porous endplates was developed and installed in the LTPT to remove the sidewall boundary layer in the vicinity of the airfoil roots. The suction flow is driven by the higher-than-atmosphere test section total pressure, and the appropriate sidewall venting configuration was developed for this particular multielement high-lift airfoil (Paschal et al.[14] described this sidewall BLC technique for a four-element airfoil). Selection of the proper venting flow rate was based on an examination of spanwise pressure variations at several chordwise locations. For the configuration tested in the present investigation, the trailing-edge flow was found to be substantially two dimensional, with a maximum spanwise variation in C_p (which was near the maximum lift), of 0.05 in the region between the flap brackets, and was measured to be even smaller at the approach angle of attack used for VG testing.[1,14,15]

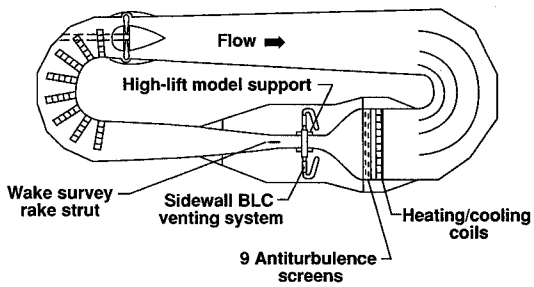

Fig. 1 NASA Langley Low-Turbulence Pressure Tunnel.

Model and Measurements

The high-lift model investigated was a McDonnell Douglas Aerospace two-dimensional, single-flap, three-element-technology airfoil.[1] The 11.55% thick model spanned the width of the test section (36 in.) and had a reference (stowed) airfoil chord c of 22 in. The slat chord ratio was 14.48% and the single-segment flap chord ratio was 30%. The model was configured for landing with a slat deflection of -30 deg and a flap deflection of 35 deg. Figure 2 shows this airfoil system in both cruise and high-lift configurations. Typically, the two-dimensional $C_{l\max}$ for this configuration was approximately 4.5 and occurred at $\alpha \approx 21$ deg. Flow separation occurred on the flap over a broad range of angle of attack below $C_{l\max}$ ($-4 \text{ deg} \le \alpha \le 18$ deg).[1] Measurements in the LTPT included lift, drag, surface pressure, mean velocity profiles in the airfoil wake, and fluctuating surface heat fluxes in a streamwise strip.

Surface pressure measurements were made with over 140 pressure taps that were connected to an electronically scanned pressure (ESP) measurement system for speedy data acquisition. Pressure orifices were located along the centerline of the model. Additional pressure taps were located in a spanwise row along (or near) the trailing edge of each airfoil element to monitor two dimensionality of the flow, as described above. Integration of the pressure measurements yielded the lift data presented here. The data are corrected for the effects of the sidewall suction system on the tunnel parameters as well as for blockage and lift interference.[13] Using the Kline and McClintock method,[16] the uncertainty in $C_{l\max}$ was calculated to be approximately ± 0.02 (or less than 1% for a $C_{l\max}$ value of 4.5). Repeatability studies confirmed this level.

Drag data were computed by integration of the static and total pressures obtained from the LTPT wake survey system. The wake profiles were measured with a 5-hole-probe rake located $1.35c$ downstream of the model. Three vertically aligned 5-hole pressure probes were attached to the probe head that was connected to the exterior traverse through an extension arm. The motor-driven traverse moved along the strut over a range of 47 in. in the vertical direction. The 5-hole pressure probes were calibrated with respect to total pressure, static pressure, and flow pitch angle over a range of pitch angles from -30 to 30 deg. On the basis of the spanwise C_p distributions and a preliminary wake profile study that covered the

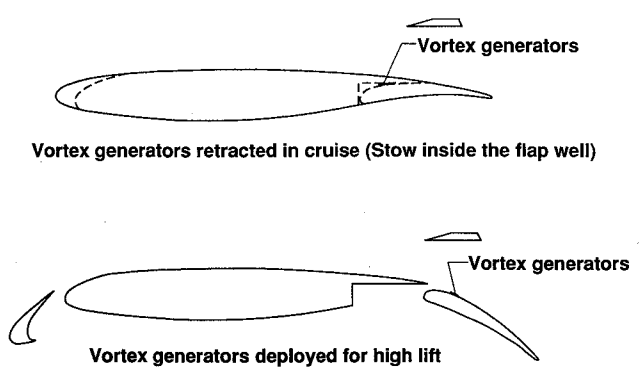

Fig. 2 Cruise and high-lift configurations with the (stowable) trapezoid-wing vortex generators.

center 44% of the model span, the flows were determined to be mostly two dimensional. Hence, the wake profile data were taken only at the centerline station. Integration of the local wake profile yielded the drag data presented here. Again, using the Kline and McClintock method,[16] the uncertainty in C_d was calculated to be approximately ± 0.0010 for the large wakes of high-lift models (e.g., 2.5% for a typical C_d value of 0.0400).[17] Repeatability studies also confirmed this level.

Previous studies in the LTPT have used arrays of surface-mounted thin-film sensors to determine transition location and extent, as well as laminar boundary-layer separation and turbulent reattachment locations.[18-20] In the present investigation, thin-film arrays were used to determine transition and to confirm separation locations on the flap. Each of the 128 sensors was driven by a constant-temperature anemometer that controlled the temperature of the film by maintaining constant resistance on the heating element. The anemometers were arranged to monitor only the time-varying (fluctuating) component of the hot-film element output voltage. Since the films were uncalibrated, the data presented here are in the form of root-mean-square (rms) values of digitized counts, which are proportional to anemometer output rms voltages (100 counts = 5.5 mV). A specially-developed software package was used for both real-time monitoring and acquisition of the output data.[21]

Based on previous separation-control studies,[10] two variants of the vane-type vortex generators were chosen for the present task: 1) a delta-wing with a height of 0.1 in., and 2) a trapezoid-wing with a height of 0.04 in. Each of these could be oriented to produce either counter-rotating (CTR) or corotating (COR) vortex pairs. The generators were arranged at alternating incident angles to produce CTR vortex pairs, and at constant incident angles to produce COR pairs. Sketches of the vortex generators are presented in Fig. 3.

The vortical layer over the flap consists of the flap boundary layer, the jet-like flow through the flap-gap, the wake of the main element, and sometimes the wake of the slat. Thus, it is difficult to define a "boundary-layer thickness" for the upper surface of the flap. For example, a velocity profile for a similar 3-element airfoil from a recent test in the LTPT[15] is shown in Fig. 4. This profile was measured at a position located 32% of the flap-chord from the flap leading edge (near the most-aft VG location in the current test), and clearly shows the flap near-wall viscous region, the gap-jet, and the main-element wake. The heights of the two vortex-generator types are shown for reference. The source of high-momentum flow that the VGs transfer toward the flap surface is the gap-jet, which peaks at about 1% of the nested-airfoil chord. The VGs are sized to occupy only 20% (trapezoid-wing) or 50% (delta-wing) of the near-wall flow beneath the velocity-peak from the flap gap. The effectiveness of such small VGs supports the results of Lin,[10] who reported that vortex generators

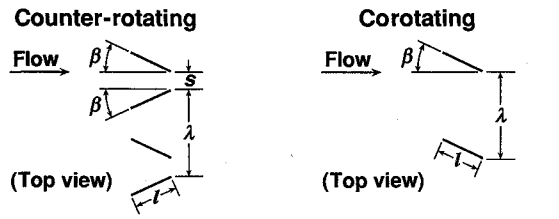

Side view of generator	h	h/c	l/h	s†/h	λ/h	β
Delta wing 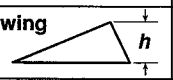	0.10"	0.0045	2.8	1.0	5.0	23°
Trapezoid wing 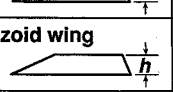	0.04"	0.0018	7.0	2.5	12.5	23°

†For counter-rotating vortex generators only

Fig. 3 Vortex generator geometry.

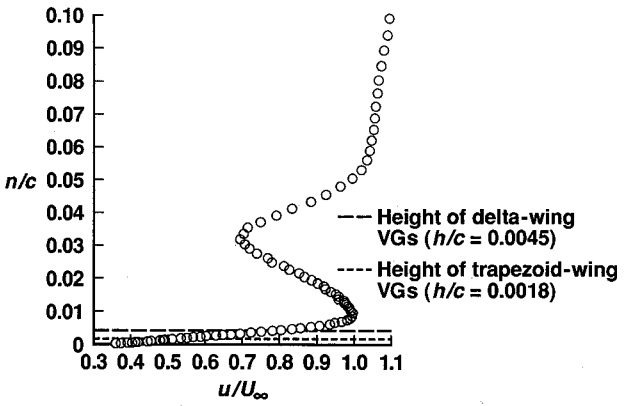

Fig. 4 Measured velocity profile from Chin et al.[15] (taken at 32% flap chord, α = 8 deg, M_∞ = 0.2, $Re_c = 9 \times 10^6$).

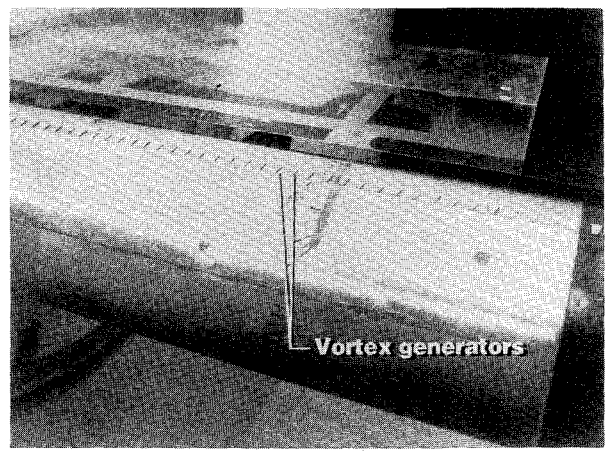

Fig. 5 Vortex generators on flap segment of McDonnell Douglas Aerospace high-lift airfoil mounted in the LTPT (view looking upstream).

as small as 0.1δ can be effective for controlling simple turbulent boundary-layer separation, and that sub-δ-scale VGs can induce effective mixing over at least three times their own heights.

Typical baseline (VG off) separation on the flap occurred at approximately 45% of the flap chord, and the vortex generators were placed at 19, 25, or 33% of the flap chord (FC). A photograph and a sketch of the flap-mounted vortex-generator installation are shown in Figs. 5 and 2, respectively. Vortex generators were also investigated on the lower surface of the main element just upstream of the backward-facing step of the flap well, and on the upper surface at 10, 25, 75, and 100% of the main-element chord (MEC).

Results and Discussion

For clarity in summarizing the results, the effectiveness of the various vortex-generator configurations tested are first compared, followed by a more detailed discussion of the observations. The relative separation-control effectiveness for all vortex-generator configurations and locations examined is summarized in Fig. 6.

At a typical landing approach condition (α = 8 deg), both the delta-wing and trapezoid-wing vortex generators were effective in alleviating boundary-layer separation on the flap when placed at 33 and 25% of the flap chord. However, when the vortex generators were moved upstream to 19% of the flap chord, only the shorter trapezoid-wing vortex generators still maintained some effectiveness. Perhaps the higher (and larger) streamwise vortices produced by the taller vortex generators migrated away from the surface, thus becoming less capable of transferring streamwise momentum all the way to the wall region. The most effective streamwise location for

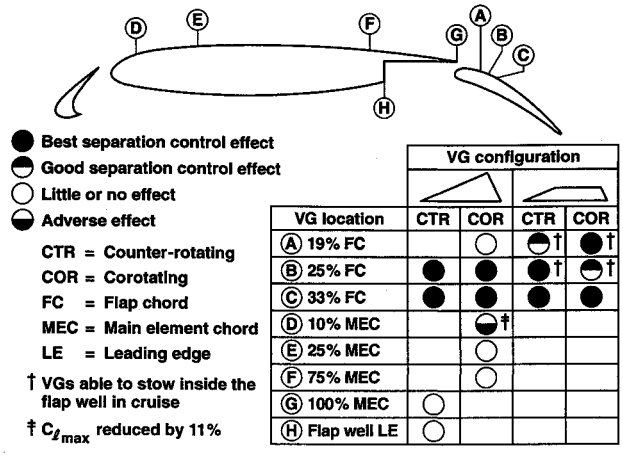

Fig. 6 Summary: relative effects of surface-mounted vortex generators for approach conditions.

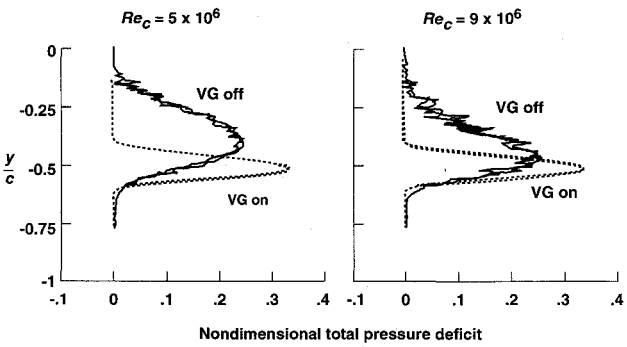

Fig. 7 Effect of vortex generators on wake profile (counter-rotating trapezoid-wing generators at 25% flap chord, α = 8 deg, M_∞ = 0.2).

the counter-rotating trapezoid-wing vortex generators was at 25% of the flap chord. The corotating trapezoid-wing vortex generators were slightly less effective than the counter-rotating configuration when placed at 25% of the flap chord. However, this trend was reversed when the corotating vortex generators were moved upstream to 19% of the flap chord. This may be due to the fact that streamwise corotating vortices generally persist longer than counter-rotating vortices in a turbulent boundary layer.[7] Delta-wing vortex generators were also investigated on the main element but yielded no significant positive effect in flap separation control and performance enhancement (e.g., increasing $C_{l_{max}}$).

As mentioned in association with Fig. 2, the low-profile, trapezoid-wing vortex generators placed at less than 26% of the flap chord could be stowed inside the flap well during cruise without any device drag penalty. Since the flow physics associated with high-lift separation control are generally similar regardless of the vortex-generator configuration, the following discussion primarily concentrates on the results associated with the low-profile, trapezoid-wing, vortex generators.

Separation-control effectiveness was evaluated in terms of lift enhancement and drag reduction. Typically, attenuating flap separation resulted in a significant narrowing of the wake of the three-element airfoil as shown in Fig. 7 for the trapezoid-wing counter-rotating vortex generators located at 25% of the flap chord. The figure shows wake profiles with and without vortex generators for both Re_c = 5 and 9 × 10^6 with α = 8 deg and M_∞ = 0.2. Flow separation on the flap resulted in a wake that covered approximately 0.5c in the vertical direction, whereas generator-induced attached flow resulted in a wake that covered approximately 0.2c. The appearance of multiple traces in the wake is due to more than one survey probe passing through the same vertical location, and this is especially noticeable for the VG-off case because of the highly unsteady nature of the separated flows. The attached-flow case had a slightly higher core-velocity than the separated-flow case. The narrowing of the wake is evidence of significant drag reduction, discussed in more detail below. There is little difference between the 5 × 10^6 and 9 × 10^6 chord-Reynolds-number profiles, except that the former had a slightly larger wake due to a slightly larger separated-flow region. Also, the VG-on wake is seen in Fig. 7 to be significantly lower than the VG-off wake, suggesting a higher downwash velocity associated with increased circulation and, therefore, enhanced lift for the VG-on case.

Separation alleviation on the flap can have a global effect on the flow over the upper surfaces of the entire high-lift system, as shown in the surface pressure results of Figs. 8 and 9 for chord Reynolds numbers of 5 × 10^6 and 9 × 10^6, respectively. It can be seen that trapezoid-wing counter-ro-

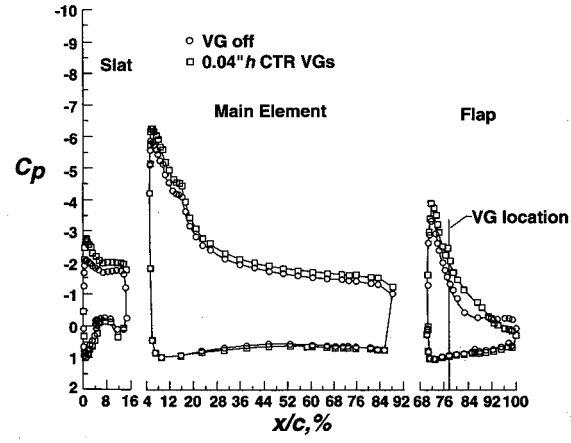

Fig. 8 Effect of vortex generators on pressure distribution (generators at 25% flap chord, α = 8 deg, M_∞ = 0.2, Re_c = 5 × 10^6).

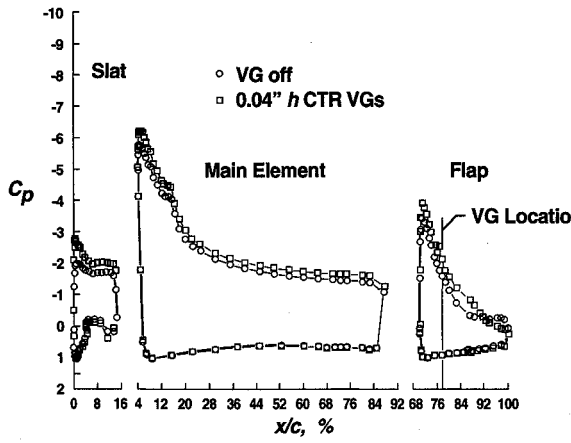

Fig. 9 Effect of vortex generators on pressure distribution (generators at 25% flap chord, α = 8 deg, M_∞ = 0.2, Re_c = 9 × 10^6).

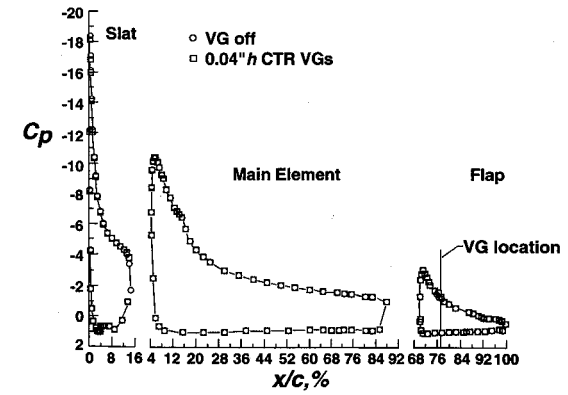

Fig. 10 Effect of vortex generators on pressure distribution (generators at 25% flap chord, α = 20 deg, M_∞ = 0.2, Re_c = 9 × 10^6).

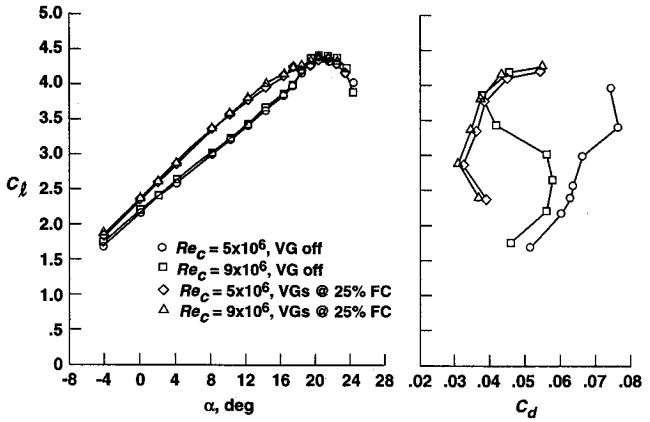

Fig. 11 Effect of vortex generators on lift and drag (counter-rotating trapezoid-wing generators, $M_\infty = 0.2$).

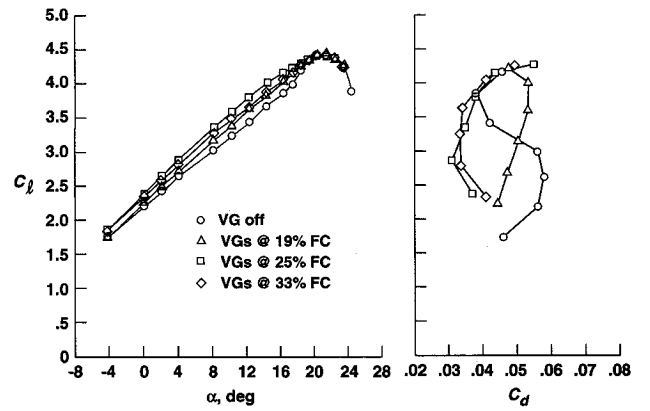

Fig. 12 Effect of vortex generators on lift and drag (counter-rotating trapezoid-wing generators, $M_\infty = 0.2$, $Re_c = 9 \times 10^6$).

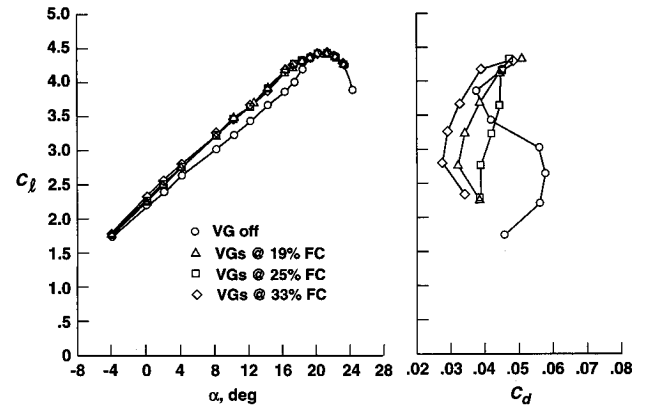

Fig. 13 Effect of vortex generators on lift and drag (corotating trapezoid-wing generators, $M_\infty = 0.2$, $Re_c = 9 \times 10^6$).

tating vortex generators mounted at 25% of the flap chord increased the suction pressure on the upper surfaces of the slat and the main element in addition to that of the flap. The increase in the suction-pressure levels resulted in significant lift enhancement at a typical approach angle of attack (i.e., $\alpha = 8$ deg). For both Reynolds numbers tested, the main-element contributed approximately 60% of the increase in lift, while the flap and the slat contributed approximately 25 and 15% of the lift enhancement, respectively. Just before airfoil stall at $\alpha \approx 21$ deg, the flow over the flap reattached, and the vortex generators no longer affected the surface pressure distribution. This is demonstrated in Fig. 10 (same VG configuration as in Fig. 9) for $\alpha = 20$ deg and a 9×10^6 chord Reynolds number. Note that the maximum suction pressure on the slat increased significantly for the near-stall case ($\alpha =$

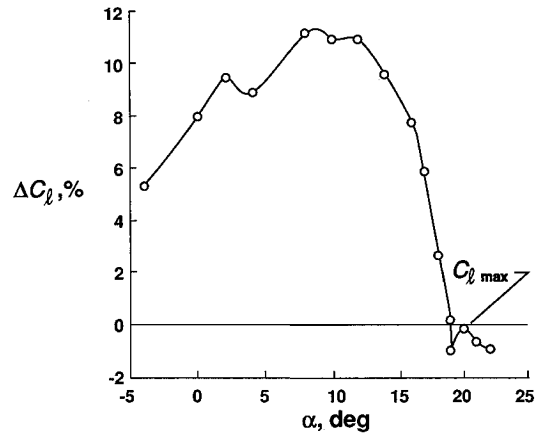

Fig. 14 Effect of vortex generators on lift coefficient (counter-rotating trapezoid-wing generators at 25% flap chord, $M_\infty = 0.2$, $Re_c = 9 \times 10^6$). $\Delta C_l = [(C_{l\,VG\,on} - C_{l\,VG\,off})/C_{l\,VG\,off}] \times 100$.

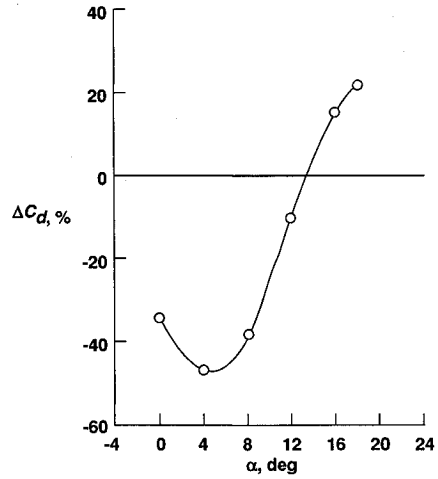

Fig. 15 Effect of vortex generators on drag coefficient (counter-rotating trapezoid-wing generators at 25% flap chord, $M_\infty = 0.2$, $Re_c = 9 \times 10^6$). $\Delta C_d = [(C_{d\,VG\,on} - C_{d\,VG\,off})/C_{d\,VG\,off}] \times 100$.

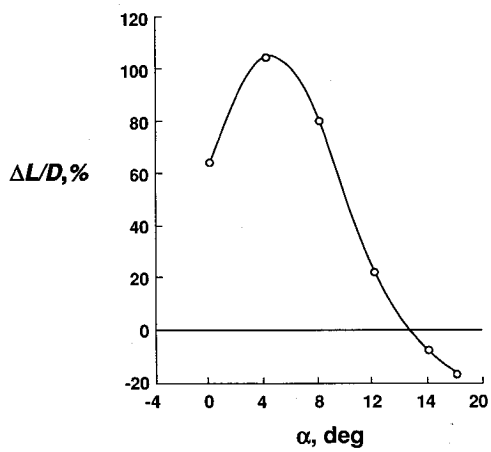

Fig. 16 Effect of vortex generators on L/D (counter-rotating trapezoid-wing generators at 25% flap chord, $M_\infty = 0.2$, $Re_c = 9 \times 10^6$). $\Delta L/D = [(L/D_{VG\,on} - L/D_{VG\,off})/(L/D_{VG\,off})] \times 100$.

20 deg) over the approach-condition case ($\alpha = 8$ deg) with or without the generators.

Lift curves and drag polars for the best-case vortex generator configuration (counter-rotating, trapezoid-wing, vortex generators located at 25% of the flap chord) with chord Reynolds numbers of 5×10^6 and 9×10^6 at Mach 0.2 are shown in Fig. 11. For the geometry tested, the beneficial effects of the VGs on both lift and drag at angles of attack

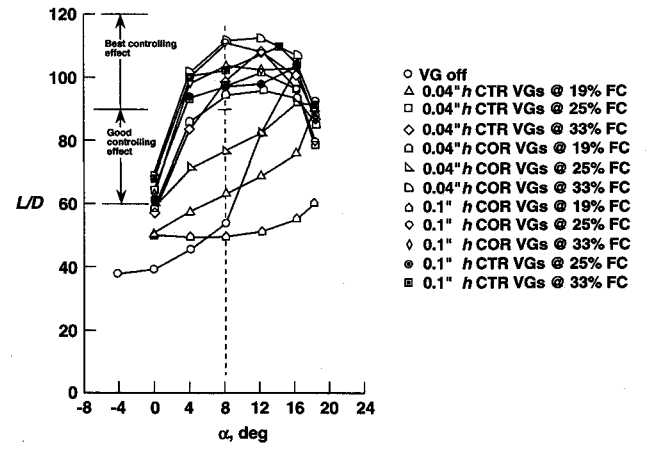

Fig. 17 Effect of vortex generator configuration and location on L/D ($M_\infty = 0.2$, $Re_c = 9 \times 10^6$).

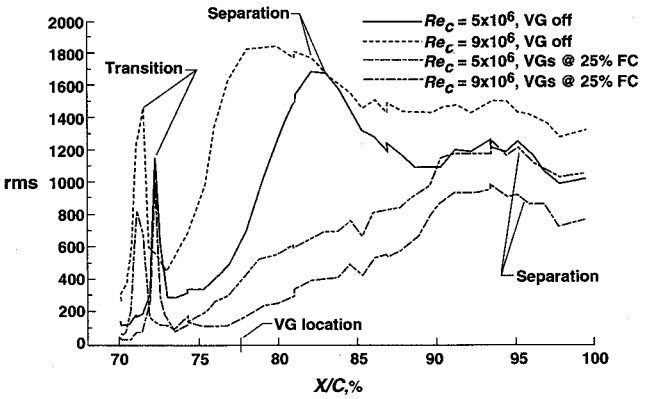

Fig. 18 Effect of vortex generators on rms thin-film anemometer output from film sensors on flap upper surface (counter-rotating trapezoid-wing generators, $\alpha = 8$ deg, $M_\infty = 0.2$).

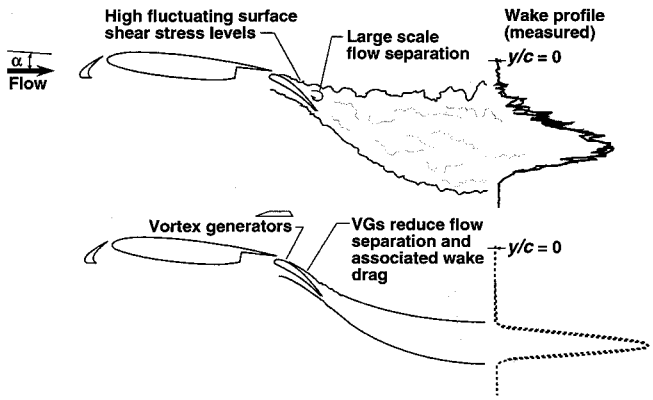

Fig. 19 Conceptual sketch of the flow physics associated with flap-mounted vortex generators at approach conditions.

below maximum lift are dramatic. The figure also shows the effect of Reynolds number for VG off on drag for 12 deg $\leq \alpha \leq$ 16 deg, where the flow moves towards reattachment only for the $Re_c = 9 \times 10^6$ case. Lift coefficients are only slightly affected by Reynolds number for the airfoil tested.

The sensitivity of lift and drag to vortex generator location is shown in Figs. 12 and 13 for counter-rotating and corotating trapezoid-wing vortex generators, respectively. Figure 12 shows that the 25% flap-chord location produced the optimum lift and drag performance for the counter-rotating case. For the corotating case, the lift curves are very similar for all three locations; however, the drag polars show that the 33% flap-chord application produced the least drag, while the 19% flap-chord application produced the next best drag performance. Note that the 19% flap-chord application would have the advantage of VGs being able to stow inside the flap well during cruise.

For the two-dimensional airfoil tested here with the counter-rotating, trapezoid-wing vortex generators at an approach angle of attack of 8 deg, the generator-induced attached flow on the flap could increase the lift on the order of 10%, reduce the drag on the order of 40%, and increase the L/D on the order of 80%, as shown in Figs. 14, 15, and 16, respectively. A summary plot of L/D curves for all flap-mounted vortex generators examined is shown in Fig. 17. Figure 6 uses information from this figure to define separation control effectiveness with $L/D \geq 90$ as having the best controlling effect, $60 \leq L/D < 90$ as having good controlling effect, and $L/D < 60$ as having little or no controlling effect at $\alpha = 8$ deg. While effective in controlling the separated flow at approach conditions, these flap-mounted vortex generators ($L/D \geq 60$) did not adversely affect the $C_{l\max}$. The $C_{l\max}$ values for these cases all came within the experimental uncertainty of 1%. As mentioned earlier, none of the delta-wing vortex generators mounted on the main element exhibited separation-control effectiveness nor $C_{l\max}$ enhancement.

In addition to improving lift and drag, the hot-film results indicated that the counter-rotating, trapezoid-wing vortex generators significantly reduced the separation-induced fluctuating shear-stress (heat flux) levels on the upper surface of the flap by as much as 70%, as indicated by the rms distributions of Fig. 18 for both 5×10^6 and 9×10^6 chord Reynolds numbers. As expected, the larger Reynolds number produced a higher level of surface heat flux fluctuations as well as moving the transition location forward. The first peak in the rms distribution indicates the transition location, while the region just downstream of the second peak indicates the approximate location of turbulent separation. The turbulent separation location was also confirmed by examining the pressure distribution on the upper surface of the flap (i.e., lack of pressure gradient). Both the pressure and rms distributions confirmed that vortex generators delayed the separation location from approximately 45% flap chord ($x/c = 0.83$) to at least 85% flap chord ($x/c = 0.95$). Using the wake profiles as a guide, a conceptual sketch (Fig. 19) of the flow physics associated with and without the flap-mounted vortex generators is illustrated. The reduction in large-scale flow separation, wake-profile size, and fluctuating shear-stress levels are directly linked.

Conclusions

Small surface-mounted vortex generators were investigated for controlling boundary-layer separation on a two-dimensional single-flap, three-element, high-lift system at near-flight Reynolds numbers and in landing configurations. The following conclusions are drawn from the present study:

1) Vortex generators as small as 0.18% of total chord, installed on the flap so as to be hidden in the flap well during cruise, can effectively control flap separation at approach conditions for high-lift configurations that have been optimized for maximum lift.

2) Both counter-rotating and corotating streamwise vortices were effective in reducing flow separation on the flap.

3) Separation alleviation on the flap significantly improved both the lift and drag performance of the high-lift airfoil at approach conditions.

4) Relative fluctuating shear-stress levels on the upper surface of the flap were reduced significantly through separation control.

5) The optimum chordwise location of the low-profile, flap-mounted, vortex generators (≈25% flap chord) allows them to be hidden inside the flap well during aircraft cruise, thus incurring no cruise drag penalty.

6) Vortex generator applications did not adversely affect the maximum lift nor lead to performance improvements for cases where the flow was already attached.

Finally, the apparent promise of micro-VGs suggests that they should be included in the design stages of an aircraft, rather than as after-design add-ons. This will require advances in turbulence modeling for complex flows, as well as a detailed turbulence documentation of the flowfield affected by micro-VGs.

Acknowledgments

The authors would like to acknowledge J. P. Stack and Aki Nakayama for the development of the hot-film measurement system used in this study. Furthermore, special thanks are extended to Wesley Goodman and all members of the LTPT and McDonnell Douglas High-Lift Technology Team for their contributions during the course of this investigation.

References

[1]Valarezo, W. O., "Topics in High-Lift Aerodynamics," AIAA Paper 93-3136, July 1993.

[2]Brune, G. W., and McMasters, J. H., "Computational Aerodynamics Applied to High-Lift Systems," *Applied Computational Aerodynamics*, edited by P. A. Henne, Vol. 125, Progress in Astronautics and Aeronautics, AIAA, Washington, DC, 1989, pp. 389–433.

[3]Woodward, D. S., Hardy, B. C., and Ashill, P. R., "Some Types of Scale Effect in Low-Speed High-Lift Flows," International Council of the Aeronautical Sciences Paper 88-4.9.3, Aug.–Sept. 1988.

[4]Kirkpatrick, D., and Woodward, D., "Priorities for High-Lift Testing in the 1990's," AIAA Paper 90-1413, June 1990.

[5]Taylor, H. D., "The Elimination of Diffuser Separation by Vortex Generators," United Aircraft Corporation Rept. R-4012-3, June 1947.

[6]Schubauer, G. B., and Spangenber, W. G., "Forced Mixing in Boundary Layers," *Journal of Fluid Mechanics*, Vol. 8, Pt. 1, 1960, pp. 10–32.

[7]Pearcey, H. H., "Shock Induced Separation and Its Prevention by Design and Boundary-Layer Control," *Boundary Layer and Flow Control,* edited by G. V. Lachman, Vol. 2, Pergamon, Oxford, England, UK, 1961, pp. 1166–1344.

[8]Nickerson, J. D., "A Study of Vortex Generators at Low Reynolds Numbers," AIAA Paper 86-0155, Jan. 1986.

[9]Bragg, M. B., and Gregorek, G. M., "Experimental Study of Airfoil Performance with Vortex Generators," *Journal of Aircraft*, Vol. 24, No. 5, 1987, pp. 305–309.

[10]Lin, J. C., "Control of Low-Speed Turbulent Separated Flow over a Backward-Facing Ramp," Ph.D. Dissertation, Old Dominion Univ., Norfolk, VA, May 1992.

[11]Wheeler, G. O., "Low Drag Vortex Generators," U.S. Patent 5058837, 1991.

[12]Kerho, M., Hutcherson, S., Blackwelder, R. F., and Liebeck, R. H., "Vortex Generators Used to Control Laminar Separation Bubbles," *Journal of Aircraft*, Vol. 30, No. 3, 1993, pp. 315–319.

[13]McGhee, R. J., Beasley, W. D., and Foster, J. M., "Recent Modifications and Calibration of the Langley Low-Turbulence Pressure Tunnel," NASA TP-2328, 1984.

[14]Paschal, K., Goodman, W., McGhee, R., Walker, B., and Wilcox, P., "Evaluation of Tunnel Sidewall Boundary-Layer-Control Systems for High-Lift Airfoil Testing," AIAA Paper 91-3243, Sept. 1991.

[15]Chin, V. D., Peters, D. W., Spaid, F. W., and McGhee, R. J., "Flowfield Measurements About a Multi-Element Airfoil at High Reynolds Numbers," AIAA Paper 93-3137, July 1993.

[16]Kline, S. J., and McClintock, F. A., "Describing Uncertainties in Single-Sample Experiments," *Mechanical Engineering*, Vol. 75, Jan. 1953, pp. 3–8.

[17]Friedman, I. P., "Calibration and Application of a New Wake Rake System for Drag Measurement of High Lift Airfoil Models," M.S. Thesis, George Washington Univ., Washington, DC, April 1991.

[18]Stack, J. P., Mangalam, S. M., and Kalburgi, V., "The Phase Reversal Phenomenon at Flow Separation and Reattachment," AIAA Paper 88-0408, Jan. 1988.

[19]Sewall, W. G., Stack, J. P., McGhee, R. J., and Mangalam, S. M., "A New Multipoint Thin-Film Diagnostic Technique for Fluid Dynamic Studies," Society of Automotive Engineers, SAE 881453, Oct. 1988.

[20]Nakayama, A., Stack, J. P., Lin, J. C., and Valarezo, W. O., "Surface Hot Film Technique for Measurements of Transition, Separation, and Reattachment Points," AIAA Paper 93-2918, July 1993.

[21]Gold, R., "Installation and Operations Manual for a Multi-Channel True RMS Measurement Data Acquisition System," Dynamic Engineering, Rept. D-389, Newport News, VA, June 1990.